Published in final edited form as:
Anticancer Drugs. 2015 February ; 26(2): 167–179. doi:10.1097/CAD.0000000000000173.

Cytotoxic and anti-angiogenic paclitaxel solubilized and permeation-enhanced by natural product nanoparticles

Zhijun Liu[a,*], **Fang Zhang**[a], **Gar Yee Koh**[a], **Xin Dong**[a], **Javoris Hollingsworth**[b], **Jian Zhang**[a], **Paul S. Russo**[b], **Peiying Yang**[c], and **Rhett W. Stout**[d]

[a]School of Renewable Natural Resources, LSU Agricultural Center, Louisiana State University

[b]Department of Chemistry, Louisiana State University

[c]Department of Cancer Biology, The University of Texas, M. D. Anderson Cancer Center

[d]School of Veterinary Medicine, Louisiana State University

Abstract

Paclitaxel (PTX) is one of the most potent intravenous chemotherapeutic agents to date, yet an oral formulation has been problematic due to its low solubility and permeability. Using the recently discovered solubilizing properties of rubusoside (RUB), we investigated this unique PTX-RUB formulation. Paclitaxel was solubilized by RUB in water to levels of 1.6 to 6.3 mg/mL at 10 to 40% weight/volume. These, nanomicellar, PTX-RUB complexes were dried to a powder which was subsequently reconstituted in physiologic solutions. After 2.5 hrs in gastric fluid 85 to 99% of PTX-RUB remained soluble, while 79 to 96% remained soluble in intestinal fluid. The solubilization of PTX was mechanized by the formation of water-soluble spherical nanomicelles between PTX and RUB with an average diameter of 6.6 nm. Compared with Taxol®, PTX-RUB nanoparticles were nearly four times more permeable in Caco-2 cell monocultures. In a side-by-side comparison with DMSO-solubilized PTX, PTX-RUB maintained the same level of cytotoxicity against three human cancer cell lines with IC_{50} values ranging from 4 nM to 20 nM. Additionally, tubular formation and migration of HUVECs were inhibited at levels as low as 5 nM. These chemical and biological properties demonstrated by the PTX-RUB nanoparticles may improve oral bioavailability and enable further pharmacokinetic, toxicologic, and efficacy investigations.

Keywords

Anti-angiogenesis; cytotoxicity; natural-product nanoparticles; permeability in Caco-2 monolayer; solubility enhancement

[*]Correspondence to: Zhijun Liu, School of Renewable Natural Resources, Louisiana State University, Baton Rouge, LA 70803 USA; Phone: 1-225-578-4214; Fax: 1-225-578-4402; zliu@agcenter.lsu.edu.

Conflicts of interest: none declared.

Introduction

Paclitaxel (PTX) is by far the most potent, naturally occurring, anti-cancer chemotherapeutic (Fig. 1) which acts by tubulin-binding thus disrupting DNA duplication [1]. Half maximal inhibitory concentrations (IC_{50}) against a wide variety of human cancer cells were reported to be in the lower nanomolar range (1 – 10 nM) for PTX. Other commonly used chemotherapeutic agents such as camptothecin achieved the same efficacy in higher nanomolar range (10 – 100 nM) [2], or in the micromolar range as seen with etoposide [3], temozolomide [4], curcumin [5, 6], and resveratrol [7]. However, PTX's pharmacological advantage is hampered by its low solubility and permeability. Paclitaxel is a non-ionizable, lipophilic, and non-polar molecule which adversely affects solubility. Additionally, PTX is a P-glycoprotein (P-gp) substrate whereby some cell types can easily pump PTX back into the extracellular space. In the biopharmaceutical classification system (BCS), paclitaxel is categorized as a BCS IV drug, the most difficult category for oral drug delivery.

PTX's solubility constraints have been addressed in Taxol® by the co-solvency approach or in Abraxane® by conjugation to a water-soluble albumin carrier. These two intravenous (IV) PTX drugs are currently prescribed to treat ovarian, breast, non-small-cell lung, small-cell lung, and head and neck cancers. PTX solubilized in Cremophor EL® or dehydrated ethanol as in Taxol® has been a frontline chemotherapeutic agent since 1992; however, hypersensitivity reactions resulting from the use of Cremophor EL® limit the treatment intensity necessary to achieve optimal clinical efficacy [8]. Solubilizing PTX by conjugation to albumin (Abraxane®) is an improvement and eliminates most of the hypersensitivity side effect. Intravenous drugs, as opposed to oral formulations, are not encumbered by gastrointestinal (GI) barriers to reach the circulation such as changing pH, mucous layers, tight junctions, and P-gp pumps.

Converting IV drugs to oral medications would offer significant advantages [9]. IV infusions generally require cancer patients to visit an outpatient facility or physicians' office for therapy. These infusions are costly, often induce nausea, and require lengthy office visits that may not available locally. Developing an oral PTX formulation has proven to be difficult. Not only is PTX difficult to solubilize, it is poorly absorbed through the intestinal epithelium. First-pass metabolism may further reduce PTX's chance to enter the systemic circulation structurally intact [10]. PTX (Abraxane®) is not suitable for oral administration because albumin, as a protein carrier, degrades in the GI tract. The Cremophor-solubilized PTX (Taxol®) is suitable for oral delivery, but PTX cannot be protected from the P-gp efflux pump and may be entrapped in Cremophor [11, 12]. Finding an effective way to solubilize and enhance oral absorption using excipients that impose minimal or no toxicity remains an elusive goal for an oral PTX formulation.

In our research on natural products, the solubilizing property of steviol glycosides, such as rubusoside, (RUB; Fig. 2) was discovered [13]. Several lipophilic chemotherapeutic compounds have been solubilized with RUB including PTX, curcumin, and etoposide [2, 3, 6]. Furthermore, RUB has demonstrated the ability to inhibit P-gp [14]. This discovery, and an initial solubilization success, prompted the present study to examine the feasibility of using RUB as a solubilizer and a P-gp inhibitor to support an oral PTX medication.

Furthermore, we examined the mechanism of solubility enhancement, stability profiles in physiologic fluids, and maintenance of indicated biological properties of the PTX-RUB nanoparticles.

Materials and methods

Chemicals

Acetonitrile and water were of HPLC grade (Mallinckrodt Baker Inc., Phillipsburg, NJ). Phosphate buffered saline or PBS (1X) was purchased from MP Biomedicals, LLC (Solon, OH). Simulated gastric fluid (SGF) and simulated intestinal fluid (SIF) were purchased from RICCA Chemical Co. (Arlington, TX). PTX with a purity of 99.5% was purchased from LC Laboratories (Woburn, MA). RUB was isolated from *Rubus suavissimus* S. Lee (Rosaceae) in our own laboratory and structurally elucidated by NMR and MS analyses [15]. The purity of RUB was determined to be > 98% by HPLC-UV. DMSO was of analytical grade (Fisher Scientific Inc., Fair Lawn NJ). The MTS (3-(4, 5-Dimethylthiazol-2-yl)-5-(3-carboxymethoxyphenyl)-2-(4-sulfophenyl)-2H-tetrazolium) solution and phenazine methosulfate were purchased from Promega Co. (Madison, WI).

HPLC protocols

An HPLC system (Waters, Milford MA) was used for the analyses. The system included a pump, an on-line degasser, a column heater compartment, an auto-sampler, and a photodiode array (PDA) detector. Empower 1 workstation software was used for equipment control as well as data acquisition and processing. All of the analyses were performed on a reverse-phase Symmetry C18 HPLC column (Waters, 150 × 4.6 mm i.d.; 5 μm) at 30 °C. For PTX detection, elution was performed with an isocratic gradient of acetonitrile and water (52:48). For RUB detection, elution was performed with an isocratic gradient of acetonitrile and water (33:67). The flow rate of the mobile phase was 1.0 mL/min and the injection volume of sample was 2 μL. The PDA detector was in a wavelength range of 200–600 nm and the selected detection wavelength was 230 nm for PTX and 215 nm for RUB. The concentrations of PTX were determined using a serial of PTX standard solutions in methanol between 100 μg/mL and 2.0 mg/mL. The concentrations of RUB were determined using a serial of RUB standard solutions in water between 10 and 100 mg/mL. All samples were centrifuged at 14,000 rpm for 10 min before injection.

Solubilization of PTX by RUB

A solvent evaporation method was used to prepare the complexes between PTX and RUB. Appropriate amounts of RUB and PTX were weighed at a ratio of 50:1 weight/weight (w/w). Then, 10 mL of absolute ethanol was added to the mixture, vortexed slightly, and heated in a water bath as needed to form a clear ethanol solution containing 2 mg/mL PTX and 100 mg/mL RUB. The ethanol solution was passed through nylon 0.45 μM filters (Whatman, Maidstone, Kent ME14 2LE, UK) to eliminate larger particles present in the solution. The ethanol solution was allowed to stand at the room temperature (22 °C) for 60 min and then was completely evaporated to a powder under reduced pressure at 50°C and agitation in a RAPIDVAP system (Labconco, Kansas City, MO). The powder of PTX and RUB (PTX-RUB) complexes was reconstituted with HPLC-grade water and centrifuged at

20,800 rcf (14,000 rpm) for 10 min. The supernatant water solution was injected and analyzed for PTX and RUB.

Characterization of the complexes formed between PTX and RUB

Determination of surface morphology—The surface morphology of the complex structure formed between PTX and RUB was studied using freeze-fracture transmission electron microscopy (FF-TEM). To do this, the PTX-RUB powder was first reconstituted in water so that the RUB concentration was 10% w/v. Freeze-fracture samples were prepared by first depositing a drop of the 10% w/v RUB-solubilized PTX water solution onto a copper planchette (BAL-TEC, Los Angeles, CA). The sample was frozen by rapid immersion into a liquid Freon (SHUR/FreezeTM Cryogen Spray, Triangle Biomedical Sciences, Durham, NC) bath, then plunged in liquid nitrogen. The vitrified sample was transferred to the sample stage, which was submerged in liquid nitrogen. After transferring the sample stage into the freeze-etching chamber of the Balzers BAF-400 apparatus, the samples were fractured at a temperature of −170 °C. Once the fractured sample was allowed to etch for about 1 min, Pt–C was deposited at a 45° angle with respect to the sample surface followed by deposition of C at a 90° angle for reinforcement. The resulting replicas were washed twice in distilled water to remove the actual sample. The replicas were collected on 400 mesh Formvar-coated grids (Electron Microscopy Sciences, Hatfield, PA) and allowed to dry overnight. TEM observations were performed with a JEOL JEM-100CX transmission electron microscope operated at 80 kV.

Particle size measurement—Particle size measurements were performed using a custom-built dynamic light scattering (DLS) apparatus equipped with a Coherent Innova 90 argon (400–800 nm) laser set to 568.2 nm. A Pacific Precision Instruments wide-range photometer/preamplifier/discriminator drives an ALV pulse shaper, which feeds an ALV-5000 digital autocorrelator. Ten percent w/v RUB-solubilized PTX water solution was transferred into clean cells via 0.22 μm Millipore Durapore Membrane filters. The temperature was controlled at 25.0 ± 0.01 °C by a circulating water bath. For each sample, five (5) repetitive runs, each of 180 sec duration, were collected. Each sample was run 5 times at 90° scattering angle with durations of 180 sec. The averaged correlation functions were analyzed with one-exponential and third-order cumulant algorithms to determine the apparent hydrodynamic diameter, D_h.

Reconstitution of PTX-RUB powder in physiologic solutions

The PTX-RUB powder was reconstituted in distilled and deionized water (control), PBS solution, SGF, and SIF. All reconstituted solutions were analyzed for pH by a pH meter (Accumet Basic, Fisher Scientific, Waltham, MA) and for the concentrations of PTX and RUB by HPLC.

Stability of the PTX-RUB nanoparticles in physiologic solutions over time and in response to dilutions

The PTX-RUB powder was reconstituted to stock solutions in three replicates in water (control), PBS solution, SGF, or SIF. Each reconstituted stock solution contained 10% w/v RUB and was then diluted by 1.3, 2, 4, or 10 fold with the same solvent. All solutions were

incubated at 37 °C. The concentrations of PTX in the diluted solutions were measured at 0.25, 2.5, 5.0, 7.5, 10, 12.5, and 24 hrs by HPLC. Results were expressed as mean ± standard deviation (SD).

Permeability assessment

Caco-2 cell culture—Caco-2 cells (ATCC® CRL-2102™) were cultured in the Dulbecco's modified Eagle's medium (DMEM) supplemented with 10% fetal bovine serum (FBS) and allowed to grow to 4×10^5 cells/mL prior to passaging. The passaged Caco-2 cells (less than 10 passages) were grown in a 75 cm^3 flask to a density of approximately 250,000 cells cm^{-2}. These cells were then trypsinized from maximally (90%) confluent Caco-2 cultures and re-suspended in DMEM. The cell suspension was transferred to a test tube and allowed to sediment to remove the debris and large cell aggregates (if any). The supernatant was then transferred to a new test tube and an aliquot of which was taken for cell count. After the cell count, the supernatant was spun down to remove the supernatant solution. These cells (at a concentration of 2.0×10^5 cells mL^{-1}) were then re-suspended in DMEM supplemented with antibiotics consisting of penicillin and streptomycin (Invitrogen Corporation, Carlsbad, CA).

Caco-2 cell monolayer culture—The assay was conducted in a 24-well plate with an insert membrane (Millipore 24-well membrane inserts with surface area of 0.31 cm^2, membrane diameter of 6.5 mm, and pore size of 3.0 μM) in each well. Before seeding these cells onto the insert membrane, the cells were mixed to minimize sediment or agglomeration. The insert membranes were pre-wetted with 0.1 mL of medium (for at least 2 min) before seeding the cells. To seed, 0.4 mL of the re-suspended cell solution was dispensed onto each insert membrane. The seeding density was 8×10^4 cells/insert. The basolateral chamber was filled with 1.0 mL of DMEM supplemented with the triple antibiotic pack consisting of penicillin, streptomycin, and amphotericin B (MP Biomedicals, Solon, OH) at 100 IU/mL, 100 μg/mL, 0.25 μg/mL, respectively. After seeding, the plate containing these inserts was incubated at 37 °C and 5% CO_2 in a humid atmosphere for 6 to 12 hrs to allow attachment of cells onto the insert membrane. After the attachment period, the apical medium containing the un-attached cells was carefully aspirated and replaced with 0.4 mL of DMEM supplemented with the antibiotics. To grow the cells for monolayer formation, medium from both the apical and basolateral sides were replaced with fresh medium every other day for up to 21 days. Cell monolayer formation and integrity were measured using an Epithelial Voltohmmeter (EVOM^2, World Precision Instruments, Sarasota, FL) for trans epithelial electrical resistance (TEER). When the values of TEER reached within the range of 250 and 650 Ohms cm^{-2}, permeability experiments were started.

Permeability assay—The culture medium was first changed 12–24 hrs before the experiment started. PTX was first solubilized in either Cremophor EL®/ethanol system (used in Taxol®) or water for PTX-RUB, then diluted with a transport buffer with pH in the range of 6.5 to 7.2. The final PTX concentration was 60 μg/mL in the transport buffer solution containing either 5.2 mg/mL Cremophor EL® and 5.0 μL/mL ethanol (PTX-Taxol®) or 3.0 mg RUB/mL (PTX-RUB). To determine the cytotoxicity of RUB as a solubilizer, drug-free RUB was assayed in separate Caco-2 cells in a concentration range of

0.6 mM (0.35 mg/mL) to 77.9 mM (50 mg/mL) following the procedure described below. This was done to determine a non-toxic concentration of RUB to Caco-2 cells that formed monolayer for permeability assay. Ranitidine and warfarin, each at 10 μM, were used as a low and high permeability control, respectively. The TEER values of each well were taken before adding the test compounds and at two hrs. For each insert, a 300 μL aliquot of test compound dissolved in transport buffer was first added to the insert (donor solution). Then 1000 μL of transport buffer was added to the well (receiver solution). The plate was then incubated at 37 °C with humidified atmosphere for 120 minutes. At the completion, 300 μL of the donor solution and 1000 μL of the receiver solution were taken and stored at −18 °C for subsequent HPLC analyses. The apical to basolateral apparent permeability (P_{app}) was calculated based on the following equation: $P_{app} = [dQ/dt] * [VA/(A*T)]$ where dQ/dt = flux from donor to receiver; VA= volume of receptor chamber (cm^3); A= area of the membrane insert (0.31 cm^2); T= Assay time (sec).

Cytotoxicity of PTX-RUB nanoparticles

Solubilization and sample preparation—To evaluate the cytotoxicity of RUB-solubilized PTX, a side-by-side comparison with DMSO-solubilized PTX was performed using a standard MTS cell viability assay. Two PTX stock solutions were prepared by either solubilizing the free PTX in absolute DMSO (PTX-DMSO) at the concentration of 23.4 μM or reconstituting the PTX-RUB powder in water to a concentration of 234.2 μM. The PTX-DMSO stock solution was diluted with culture medium by 10 fold while the PTX-RUB stock solution by 100 fold so that both assay solutions contained identical 2.34 μM PTX. These assay solutions were further serially diluted to a range of 0.91 nM and 117 nM by either culture medium with 1% v/v DMSO (for PTX-DMSO) or 0.01% w/v RUB (for PTX-RUB).

Cell culture—The human prostate carcinoma (DU 145), breast carcinoma (MDA-MB-231), and human colon adenocarcinoma (HT-29) cell lines were obtained from the American Type Culture Collection (ATCC) and maintained at 37 °C in a humidified atmosphere with 5% CO_2. Cells were cultured in DMEM supplemented with 10% FBS, N-2-Hydroxyethylpiperazine-N´-2-ethanesulfonic Acid (HEPES), penicillin-streptomycin, sodium pyruvate, L-glutamine, and non-essential amino acids. All cell culture materials were purchased from Invitrogen Corporation (Carlsbad, CA).

In vitro cell viability assays: Cell viability was tested using the MTS assay. HT-29, DU145, or MDA-MB-231 cells were added to 96-well plates at 1×10^4 cells/well, respectively, and allowed to adhere overnight. The cells were then treated with PTX-RUB nanoparticle solutions prepared above ranging from 0.91 nM to 117 nM of PTX in triplicate wells and incubated at 37 °C for 96 hrs. On day four, a 20 μL aliquot of MTS solution premixed with phenazine methosulfate was added directly to each well and the plate was incubated at 37 °C for another 1 to 2 hrs. Absorbance was measured at a wavelength of 490 nm using a Bio-Rad Microplate Reader (Hercules, CA). Percent viability was calculated as cell viability relative to vehicle-treated control (100%). The IC_{50} values were the average of at least two independent experiments.

Angiogenesis of human umbilical vascular endothelial cells

Tube formation—The human umbilical vein endothelial cells (HUVECs) were purchased from the American Type Culture Collection (ATCC # CRL-1730, Manassas, Virginia). HUVECs were grown in M199 media containing 20% FBS, 30 μg/ml endothelial cell growth supplements, 4 mM L-glutamine, 100 U/mL penicillin, and 100 μg/mL streptomycin. Cells were incubated at 37 °C in a humidified atmosphere of 5% CO_2. They were treated with PBS containing 1% DMSO or containing RUB as the vehicle controls and various concentrations of PTX in either DMSO or RUB system for 24 hrs. Tube formation was recorded under a microscope connected to a digital camera.

Migration—Migration of HUVECs was assessed by scraping a zone free of HUVECs. After 6 hrs of incubation with vehicle controls or various concentrations of PTX in DMSO or RUB system, digital images were taken under a microscope. Clear zones indicated a complete inhibition of HUVEC migration whereas invasion of neighboring HUVECs indicated partial or no inhibition.

Statistical analysis

All data were analyzed using the paired Student's T-test or one-way ANOVA followed by Tukey Post-hoc test (SAS, Cary, NC). Data were expressed as mean ± SE (standard error) unless otherwise specified. Significance of all tests was set at $P \leq 0.05$.

Results

Solubilization of PTX by RUB

Using the organic solvent evaporation method, a powder was obtained that contained 2% w/w PTX and 98% w/w RUB. This powder was instantly and completely reconstituted to water solutions of various percentages of RUB. Corresponding to 1%, 2.5%, 5%, 7.0%, 9.1%, 20%, and 40% w/v RUB, PTX was solubilized to 0.08, 0.27, 0.66, 1.10, 1.57, 3.54, and 6.26 mg/mL (Table 1), respectively. pH values of the reconstituted PTX-RUB water solutions increased slightly from 5.7 to 6.2 as the concentrations of both PTX and RUB increased. The volume of water solutions increased by 0 (no change), 1, 4, 7, 9, 11, and 15% after the addition of PTX-RUB powder by the amounts of 1, 2.5, 5, 7.5, 10, 20, and 40% w/v, respectively. There were no unknown peaks detected in the chromatogram (Fig. 3), an indication of structural stability of both the drug and the solubilizer during the solubilization process. By reconstituting the powder to a 40% RUB water solution, a PTX concentrate was made. This concentrate contained 6.3 mg/mL PTX and was clear and transparent (Fig. 4).

Reconstitutability of the PTX-RUB nanoparticles in physiologic solutions

The PTX-RUB nanoparticulate powder was reconstituted in water, PBS saline, SGF, or SIF. In the reconstituted solutions, PTX and RUB concentrations were consistent with the expected values (Table 2) based on the knowledge of PTX content in the powder. The pH of the reconstituted water solutions depended on the type of media. pH values were 6.20, 7.21, 1.12, and 5.75, respectively, for water, PBS saline, SGF, and SIF.

Size and shape of the PTX-RUB nanoparticles in a water solution

Based on the linear behavior of the semilogarithmic plot shown in Fig. 5A, the PTX-RUB complexes were confirmed as monodisperse. The measured apparent hydrodynamic diameter, D_h, was 6.6 ± 0.4 nm (Fig. 5B). Although conclusive evidence about the size and dispersity of the solution was obtained from the semilogarithmic plot of the autocorrelation function, further distribution analyses reaffirmed these findings (data not shown). Fig. 6 shows the FF-TEM images of a reconstituted PTX-RUB nanoparticle water solution, in which the numerous spherical dark spots were believed to be the complex particles formed between PTX and RUB in the nanometer range, in agreement with the DLS results.

Stability of the PTX-RUB nanoparticles in physiologic solutions over time and in response to dilutions

Stock solutions were prepared by reconstituting PTX-RUB powder in water, PBS saline, SGF, and SIF, respectively. These reconstituted transparent stock solutions contained approximately 10% w/v RUB and 1.6 mg/mL of PTX. When the respective stock solutions were diluted by a factor of 1.3, 2, 4 and 10 with a respective medium, RUB concentrations were respectively 7.5%, 5%, 2.5%, and 1% w/v with no observable precipitation at the outset. Subsequently, the PTX concentrations declined over time in all four dilutions, as well as the stock physiologic solutions (Fig. 7). PTX-RUB complexes experienced the least precipitation in water (Fig. 7A) and the most in PBS saline (Fig. 7B), whereas results were in-between for SGF (Fig. 7C) or SIF (Fig. 7D). In the stock solutions (10% RUB), which were prepared from direct reconstitution of the PTX-RUB powder, PTX precipitated from 1.2 to 6.8% at 2.5 hrs and ranged from 9.4 to 30.3% by 24 hrs. At lower RUB concentrations (1 to 7.5%), which were prepared by dilution of the stock solutions, PTX precipitated at a higher rate where as much as 64.7% precipitated out by 24 hrs in the PBS/2.5% RUB solution. In contrast to PTX, RUB concentrations remained unchanged in all physiologic solutions over a period of 24 hrs (Fig. 8)

Permeability across Caco-2 cell monolayer

PTX in the RUB nanoparticles was more permeable through the monolayer than that demonstrated for the PTX-Taxol® system. PTX-RUB displayed a permeability coefficient of 3.83, approximately 3.5 times the rate of PTX-Taxol® (Table 3). The PTX in the PTX-RUB nanoparticles was fully solubilized by a single natural compound RUB at 4.7 mM (3 mg/mL) in water without any organic solvents whereas the PTX in the Taxol® formulation was fully solubilized by the combination of Cremophor El® (5.2 mg/mL) and ethanol (5.0 μL/mL). At 4.7 mM or lower, RUB did not affect cell viability of Caco-2 monolayers (Fig. 9). RUB alone started to reduce cell viability at a concentration of 4.7 mM and completely inhibited cell growth at 19.5 mM with an IC_{50} value of 10.4 mM (6.7 mg/mL).

Cytotoxicity of the PTX-RUB nanoparticles

RUB-solubilized PTX demonstrated IC_{50} values of 3.77 nM, 20.22 nM, and 15.49 nM against HT-29, MDA-MB-231, and DU-145 human cancer cells respectively. Maximal inhibition of cancer cell growth was achieved for all three cell lines by the PTX-RUB nanoparticles at a PTX concentration of 117 nM (Fig. 10). RUB alone (vehicle) had no

effect on the viability of any cell line. No differences in cancer cell inhibition could be demonstrated between the PTX-DMSO and PTX-RUB solutions (Table 4).

Anti-angiogenic properties of the PTX-RUB nanoparticles

HUVECs under control conditions developed healthy, normal, tubes. The 1% DMSO or RUB vehicle had no effect on the tube formation or cell migration. The addition of solubilized PTX to the cell culture, however, resulted in visible effects on the formation of tubules and on cell migration. PTX, starting at the 5 nM concentration and regardless of DMSO-solubilized or RUB-solubilized system, disrupted the completion of tube formation (Fig. 11A) and prevented cell migration (Fig. 11B). These inhibitory effects became more profound as the concentrations of PTX increased to 25 nM and 50 nM.

Discussion

Various strategies have been used to solubilize paclitaxel but here we report solubilization of PTX with the natural product RUB. Solubility levels of 1.6 mg/mL to 6.3 mg/mL of PTX in physiologic solutions were achieved by the use of 100 mg/mL to 400 mg/mL of RUB. RUB is more efficient at solubilization of PTX than the Cremophor EL®/absolute ethanol combination. RUB at 400 mg/mL can solubilize PTX to 6 mg/mL, the same level achieved by the use of 527 mg/mL Cremophor EL® and 497 μL/mL absolute ethanol as used in Taxol®. The ability to form a powder from the RUB/PTX solution and its subsequent reconstitutability expand the range of dosage forms possible over that seen with non-aqueous liquid formats. Solubilization of PTX has been extensively studied using conventional techniques, initially to replace the toxic Cremophor EL®. Recently, emphasis has shifted to developing oral PTX formulations. Three major strategies for oral delivery of PTX have been adopted and are summarized in Table 5. Recently polymeric nanoparticles of various types have become a major strategy for pharmaceutical delivery whereby PTX was loaded into lipophilic nanoparticle cores. Various types of nanoparticle cores have been constructed to host the lipophilic PTX, such as poly(DL-lactide-co-glycolide) and poly(DL-lactide) [25], d-α-tocopheryl polyethylene glycol 1000 succinate [26, 27], β-casein (β-CN) micelles [28], gelatin [29], and lipid nanocapsules [9, 30]. These constructed nanoparticles are not water-soluble and must be coated and solubilized with surfactants such as polyethylene glycol (PEG), polysorbate 80 (Tween® 80), and Solutol® for oral delivery. Some polymeric nanoparticle cores are constructed with built-in solubilizing factors through conjugating the core to a solubilizing agent (e.g., PEG). In these cases, PTX-loaded nanoparticle cores require no additional solubilizing agent [19–23, 31]. Co-solvency is another strategy used to create water-soluble formulations for oral delivery of PTX, as seen with Taxol®. Complexation, such as the use of cyclodextrins, is a third strategy employed to solubilize PTX for oral delivery [32–34].

In comparison with conventional nanocore-surfactant approaches, RUB serves as a nanocore and a solubilizer for the PTX-RUB nanoparticles. In the current study we demonstrated the feasibility of RUB as a PTX solubilizer. PTX was molecularly dispersed into RUB at a ratio of 1:50 by weight. We achieved a solubility level of 6.3 mg/mL of PTX by reconstituting the powder into a clear and transparent water solution as a PTX concentrate (Fig. 4). At 6.3

mg/mL the solubility of PTX is enhanced nearly 18,000 fold over that seen in water (350 ng/mL) and 120 times the minimum requirement of 52 μg/mL for pharmaceutical drugs based on a 1 mg/kg clinical dose with average permeability [35].

The mechanism of solubilization of PTX by RUB appears to be the formation of water-soluble micellar nanoparticles between PTX and RUB, similar to the mechanism observed for the micellar nanoparticles formed between curcumin and RUB along with etoposide and RUB [3, 6]. Along with a similar solubilization mechanism, particle size among the three compounds is also similar (paclitaxel, 7 nm; curcumin, 8 nm; etoposide, 6 nm). It is noticeable that the PTX-RUB nanoparticles observed under TEM (Fig. 6) were not one size, as the DLS found (Fig. 5). It is possible that during sample preparations for TEM imaging, nanoparticles may have overlaid and formed aggregates. Compared with existing formulations developed for PTX, the PTX-RUB nanoparticles were the smallest size while in solution (Table 5). Particle size has been implicated as an important factor affecting cellular entry and transport. In a study on the chemotherapeutic agent etoposide, a particle size of 105 nm was shown to sustain plasma etoposide levels higher and longer than that of 160 nm etoposide-loaded PLGA nanoparticles [36]. It is generally recognized that particle sizes of < 150 nm are favored for tumor penetration [37]. Conventional nanoparticle development has sought to produce smaller, rather than larger, particle sizes in the range of 10 to 100 nm. Nonetheless, the biological implications of nanoparticulate size remains poorly defined. PTX-RUB nanoparticles were shown to enter cancer cell cultures with similar efficacy as PTX-DMSO [2], possibly due to their small size (Table 5). Whether the smaller particle size alone will translate to better pharmacokinetic profiles and efficacy remains to be elucidated.

Solubility and stability are two important factors for adequate drug exposure. Our stability profiles demonstrated that at 2.5 hours 82% to 99% of the PTX-RUB nanoparticles remained solubilized in gastric fluid while 79% to 96% remained solubilized in the intestinal fluid depending on the RUB concentration (from 1 to 10% w/v). In oral medications, major intestinal absorption takes place within the first two hours after consumption. During these two hours, PTX was released from the PTX-RUB nanoparticles at various rates depending on the properties of physiologic solutions. Less release was seen in the acidic gastric fluid than the neutral intestinal fluid. While PBS and intestinal fluid have similar pH values, the release of PTX from the PTX-RUB nanoparticles in intestinal fluid was approximately half of that seen in PBS at 24 hours. Although the reason is not clear, the salt in the PBS solution may have triggered a release of PTX from the nanoparticles. The RUB concentrations remained constant over the same period, indicating RUB nanoparticles maintained their integrity under these conditions. How RUB molecules interact among themselves and whether there were subtle changes in configuration remains to be demonstrated.

Ultimately, plasma drug levels have to reach a therapeutic range to be efficacious. Our cell viability assay demonstrated that PTX was detrimental to half of the dividing cancerous cells, for all three cells lines, at a level ranging from 4 to 20 nM (Table 4). Therefore, we suspect plasma PTX levels may need to reach these levels to exert a therapeutic effect. The plasma PTX concentration starting at 5 nM would also be effective in preventing angiogenesis (Fig. 11). Further testing will be required to determine if these *in vitro* results

translate to *in vivo* efficacy. The PTX-RUB nanoparticles demonstrated in this study will facilitate future *in vivo* toxicology, pharmacokinetics, and efficacy studies.

In addition to addressing the PTX solubility issue, RUB appears to be capable of overcoming some cell permeability barriers. P-gp is one of the most well recognized efflux transporters [38]. It is present in many tissues including the intestine, brain, liver and kidney. RUB itself is a weak P-gp inhibitor compared to the inhibitor verapamil. At 1.6 mM (1 mg/mL) RUB inhibited P-gp by 59% whereas verapamil completely blocked P-gp at only 100 μM [14]. The P-gp inhibitory effects of RUB at other doses (e.g., 3 mg RUB/mL used in the Caco-2 assay) are unknown and need to be determined in future experiments. Whether cell penetration by PTX-RUB is by P-gp inhibition alone or some other mechanisms such as nanoparticulation or smaller particle size is hard to define. Regardless, our PTX-RUB nanoparticles facilitated the passage of PTX across the Caco-2 cell monolayer and predict 60% intestinal absorption [39] whereas PTX in the Taxol® formulation was not permeable, in agreement with other findings [9, 10, 30]. Apparently, solubility was not the issue affecting permeability as PTX remained soluble in both systems (Taxol® or PTX-RUB). In clinical trials, converting Taxol® to an oral medication was attempted in cancer patients and a P-gp inhibitor, such as cyclosporine or verapamil, was required to improve PTX bioavailability [9, 40]. Long-term uses of these inhibitors that are immunosuppressive and calcium channel blockers may present safety concerns. The oral paclitaxel formulation (Paxoral®) developed by IVAX Research needs cyclosporine co-administration to increase bioavailability [41] and thus faces the same dilemma. Loading paclitaxel in lipid nanoparticles and subsequently solubilized by Solutol® HS15 increased oral bioavailability 3-fold over Taxol® but huge inter-animal variability exists [9]. In addition to the low absorption, Cremophor EL® in the Taxol® formulation causes hypersensitivity reactions [8, 42, 43]. Although Cremophor may not be intestinally absorbed thus avoiding possible systemic allergic reactions, Cremophor can cause GI toxicity [40].

Compared with existing nanoparticle formulations, a self-associating solubilizer and permeation-enhancing food compound, RUB, appears to hold greater promise. Although existing nanoparticle formulations appear to be conceptually sound, succeeding in both delivery efficiency and safety may require major advancements of nanotechnology to adequately address their limitations. These include the insolubility of the nanoparticles which often requires an effective solubilizing ingredient for “coating” [44], the complexity (e.g., multiple layers) and concomitant stability and manufacturing cost, and the potential toxicity of synthetic ingredients.

The PTX-RUB nanoparticles were bioavailable to the cancer cells. In our previous study, cellular uptake of PTX in the PTX-RUB nanoparticles was found [2]. A side-by-side comparison of the cytotoxicity of PTX prepared in absolute DMSO or RUB water solution showed precisely that the cytotoxic and anti-angiogenic properties of the drug compound was fully maintained, regardless of solubilizing systems.

In summary, this study demonstrated that paclitaxel can be solubilized by a natural compound, RUB, to a level of 6.3 mg/mL that is equivalent to the Taxol® (6 mg/mL) but without the use of Cremophor and ethanol. PTX and RUB formed soluble nanoparticles with

diameter of approximately 7 nm. The PTX-RUB nanoparticles can be made into a powder, which then can be instantly and completely reconstituted in physiologic solutions. In a Caco-2 permeability assay, PTX in the PTX-RUB nanoparticles was over 3 times more permeable than Taxol®. When cultured with human cancer cells, cytotoxicity of the PTX-RUB nanoparticles was fully maintained showing no statistical differences with that of DMSO-solubilized PTX. Moreover, similar anti-angiogenic activity between the PTX-RUB nanoparticles and DMSO-solubilized paclitaxel was displayed. These promising results warrant further study of the PTX-RUB nanoparticles for the determination of oral bioavailability and anti-tumor efficacy.

Acknowledgments

The content is solely the responsibility of the authors and does not necessarily represent the official views of the National Cancer Institute or the National Institutes of Health. We would like to thank Karen McDonough in the LSU Agricultural Center Cell Culture Core for providing all cell lines and for technical assistance with cell culture. We also thank Dr. Li Ding of China Pharmaceutical University for the generosity of sharing his expertise in instrumental analysis.

Source of funding: This research was supported by the Grant Number 1R21CA167255-01 from the National Cancer Institute to Liu Z, and partially by the Technology Transfer fund of the LSU AgCenter.

Abbreviations

DLS	dynamic light scattering
DMEM	Dulbecco’s modified Eagle’s medium
DMSO	dimethyl sulfoxide
FBS	fetal bovine serum
FF-TEM	freeze-fracture transmission electron microscopy
HUVECs	human umbilical vein endothelial cells
PBS	phosphate buffered saline
PEG	polyethylene glycol
P-gp	p-glycoprotein
PTX	paclitaxel
RUB	rubusoside
SGF	simulated gastric fluid
SIF	simulated intestinal fluid

References

1. Kavallaris M. Microtubules and resistance to tubulin-binding agents. Nat Rev Cancer. 2010; 10:194–204. [PubMed: 20147901]
2. Jeansonne DP, Koh GY, Zhang F, Kirk-Ballard H, Wolff L, Liu D, et al. Paclitaxel-induced apoptosis is blocked by camptothecin in human breast and pancreatic cancer cells. Oncol Rep. 2011; 25:1473–1480. [PubMed: 21331447]

3. Zhang F, Koh GY, Hollingsworth J, Russo PS, Stout RW, Liu Z. Reformulation of etoposide with solubility-enhancing rubusoside. Int J Pharm. 2012; 434:453–459. [PubMed: 22698860]
4. Sankar A, Thomas DG, Darling JL. Sensitivity of short-term cultures derived from human malignant glioma to the anti-cancer drug temozolomide. Anticancer Drugs. 1999; 10:179–185. [PubMed: 10211548]
5. Thomas SL, Zhong D, Zhou W, Malik S, Liotta D, Snyder JP, et al. EF24, a novel curcumin analog, disrupts the microtubule cytoskeleton and inhibits HIF-1. Cell Cycle. 2008; 7:2409–2417. [PubMed: 18682687]
6. Zhang F, Koh GY, Jeansonne DP, Hollingsworth J, Russo PS, Vicente G, et al. A novel solubility-enhanced curcumin formulation showing stability and maintenance of anticancer activity. J Pharm Sci. 2011; 100:2778–2789. [PubMed: 21312196]
7. Bertini S, Calderone V, Carboni I, Maffei R, Martelli A, Martinelli A, et al. Synthesis of heterocycle-based analogs of resveratrol and their antitumor and vasorelaxing properties. Bioorg Med Chem. 2010; 18:6715–6724. [PubMed: 20728369]
8. Lal LS, Gerber DL, Lau J, Dana W. Retrospective evaluation of weekly paclitaxel hypersensitivity reactions reported utilizing an electronic medical record system at a tertiary cancer center. Support Care Cancer. 2009; 17:1311–1315. [PubMed: 19184123]
9. Peltier S, Oger JM, Lagarce F, Couet W, Benoit JP. Enhanced oral paclitaxel bioavailability after administration of paclitaxel-loaded lipid nanocapsules. Pharm Res. 2006; 23:1243–1250. [PubMed: 16715372]
10. Rochat B. Role of cytochrome P450 activity in the fate of anticancer agents and in drug resistance: focus on tamoxifen, paclitaxel and imatinib metabolism. Clin Pharmacokinet. 2005; 44:349–366. [PubMed: 15828850]
11. Malingre MM, Schellens JH, Van Tellingen O, Ouwehand M, Bardelmeijer HA, Rosing H, et al. The co-solvent Cremophor EL limits absorption of orally administered paclitaxel in cancer patients. Br J Cancer. 2001; 85:1472–1477. [PubMed: 11720431]
12. Bardelmeijer HA, Ouwehand M, Malingre MM, Schellens J, Beijnen JH, van Tellingen O. Entrapment by Cremophor EL decreases the absorption of paclitaxel from the gut. Cancer Chemother Pharmacol. 2002; 49:119–125. [PubMed: 11862425]
13. Liu, Z. Diterpene glycosides as natural solubilizers. US Patent Application PCT/USA2009. 040324. 2009.
14. Liu, Z. Water soluble drug-solubilizer powders and their Uses. US Patent Application PCT/USA2010. 52786. 2010.
15. Chou G, Xu SJ, Liu D, Koh GY, Zhang J, Liu Z. Quantitative and fingerprint analyses of Chinese sweet tea plant (Rubus suavissimus S. Lee). J Agric Food Chem. 2009; 57:1076–1083. [PubMed: 19138116]
16. Le Garrec D, Gori S, Luo L, Lessard D, Smith DC, Yessine MA, et al. Poly(N-vinylpyrrolidone)-block-poly(D,L-lactide) as a new polymeric solubilizer for hydrophobic anticancer drugs: in vitro and in vivo evaluation. J Control Release. 2004; 99:83–101. [PubMed: 15342183]
17. Zhang X, Jackson JK, Burt HM. Development of amphiphilic diblock copolymers as micellar carriers of taxol. Int J Pharm. 1996; 132:195–206.
18. Lee SC, Huh KM, Lee J, Cho YW, Galinsky RE, Park K. Hydrotropic polymeric micelles for enhanced paclitaxel solubility: in vitro and in vivo characterization. Biomacromolecules. 2007; 8:202–208. [PubMed: 17206808]
19. Dabholkar RD, Sawant RM, Mongayt DA, Devarajan PV, Torchilin VP. Polyethylene glycol-phosphatidylethanolamine conjugate (PEG-PE)-based mixed micelles: some properties, loading with paclitaxel, and modulation of P-glycoprotein-mediated efflux. Int J Pharm. 2006; 315:148–157. [PubMed: 16616818]
20. Berlin JM, Leonard AD, Pham TT, Sano D, Marcano DC, Yan S, et al. Effective drug delivery, in vitro and in vivo, by carbon-based nanovectors noncovalently loaded with unmodified Paclitaxel. ACS Nano. 2010; 4:4621–4636. [PubMed: 20681596]
21. Han LM, Guo J, Zhang LJ, Wang QS, Fang XL. Pharmacokinetics and biodistribution of polymeric micelles of paclitaxel with Pluronic P123. Acta Pharmacol Sin. 2006; 27:747–753. [PubMed: 16723095]

22. Liu F, Park JY, Zhang Y, Conwell C, Liu Y, Bathula SR, et al. Targeted cancer therapy with novel high drug-loading nanocrystals. J Pharm Sci. 2010; 99:3542–3551. [PubMed: 20564383]
23. Li H, Huo M, Zhou J, Dai Y, Deng Y, Shi X, et al. Enhanced oral absorption of paclitaxel in N-deoxycholic acid-N, O-hydroxyethyl chitosan micellar system. J Pharm Sci. 2010; 99:4543–4553. [PubMed: 20845453]
24. Varma MV, Panchagnula R. Enhanced oral paclitaxel absorption with vitamin E-TPGS: effect on solubility and permeability in vitro, in situ and in vivo. Eur J Pharm Sci. 2005; 25:445–453. [PubMed: 15890503]
25. Mu L, Feng SS. A novel controlled release formulation for the anticancer drug paclitaxel (Taxol): PLGA nanoparticles containing vitamin E TPGS. J Control Release. 2003; 86:33–48. [PubMed: 12490371]
26. Dong Y, Feng SS. Poly(d,l-lactide-co-glycolide)/montmorillonite nanoparticles for oral delivery of anticancer drugs. Biomaterials. 2005; 26:6068–6076. [PubMed: 15894372]
27. Zhao L, Feng SS. Enhanced oral bioavailability of paclitaxel formulated in vitamin E-TPGS emulsified nanoparticles of biodegradable polymers: in vitro and in vivo studies. J Pharm Sci. 2010; 99:3552–3560. [PubMed: 20564384]
28. Shapira A, Assaraf YG, Epstein D, Livney YD. Beta-casein nanoparticles as an oral delivery system for chemotherapeutic drugs: impact of drug structure and properties on co-assembly. Pharm Res. 2010; 27:2175–2186. [PubMed: 20703895]
29. Yeh TK, Lu Z, Wientjes MG, Au JL. Formulating paclitaxel in nanoparticles alters its disposition. Pharm Res. 2005; 22:867–874. [PubMed: 15948030]
30. Roger E, Lagarce F, Garcion E, Benoit JP. Lipid nanocarriers improve paclitaxel transport throughout human intestinal epithelial cells by using vesicle-mediated transcytosis. J Control Release. 2009; 140:174–181. [PubMed: 19699246]
31. Kim S, Kim JY, Huh KM, Acharya G, Park K. Hydrotropic polymer micelles containing acrylic acid moieties for oral delivery of paclitaxel. J Control Release. 2008; 132:222–229. [PubMed: 18672013]
32. Agueros M, Zabaleta V, Espuelas S, Campanero MA, Irache JM. Increased oral bioavailability of paclitaxel by its encapsulation through complex formation with cyclodextrins in poly(anhydride) nanoparticles. J Control Release. 2010; 145:2–8. [PubMed: 20347897]
33. Bilensoy E, Gurkaynak O, Ertan M, Sen M, Hincal AA. Development of nonsurfactant cyclodextrin nanoparticles loaded with anticancer drug paclitaxel. J Pharm Sci. 2008; 97:1519–1529. [PubMed: 17705171]
34. Bouquet W, Ceelen W, Fritzinger B, Pattyn P, Peeters M, Remon JP, et al. Paclitaxel/beta-cyclodextrin complexes for hyperthermic peritoneal perfusion - formulation and stability. Eur J Pharm Biopharm. 2007; 66:391–397. [PubMed: 17240125]
35. Lipinski CA. Drug-like properties and the causes of poor solubility and poor permeability. J Pharmacol Toxicol Methods. 2000; 44:235–249. [PubMed: 11274893]
36. Yadav KS, Chuttani K, Mishra AK, Sawant KK. Effect of Size on the Biodistribution and Blood Clearance of Etoposide-Loaded PLGA Nanoparticles. PDA J Pharm Sci Technol. 2011; 65:131–139. [PubMed: 21502074]
37. Chen ZG. Small-molecule delivery by nanoparticles for anticancer therapy. Trends Mol Med. 2010; 16:594–602. [PubMed: 20846905]
38. Wakasugi H, Yano I, Ito T, Hashida T, Futami T, Nohara R, et al. Effect of clarithromycin on renal excretion of digoxin: interaction with P-glycoprotein. Clin Pharmacol Ther. 1998; 64:123–128. [PubMed: 9695727]
39. Press B, Di Grandi D. Permeability for intestinal absorption: Caco-2 assay and related issues. Curr Drug Metab. 2008; 9:893–900. [PubMed: 18991586]
40. Koolen SL, Beijnen JH, Schellens JH. Intravenous-to-oral switch in anticancer chemotherapy: a focus on docetaxel and paclitaxel. Clin Pharmacol Ther. 2010; 87:126–129. [PubMed: 19924122]
41. Helgason HH, Kruijtzer CM, Huitema AD, Marcus SG, ten Bokkel Huinink WW, Schot ME, et al. Phase II and pharmacological study of oral paclitaxel (Paxoral) plus ciclosporin in anthracycline-pretreated metastatic breast cancer. Br J Cancer. 2006; 95:794–800. [PubMed: 16969354]

42. Poirier VJ, Hershey AE, Burgess KE, Phillips B, Turek MM, Forrest LJ, et al. Efficacy and toxicity of paclitaxel (Taxol) for the treatment of canine malignant tumors. J Vet Intern Med. 2004; 18:219–222. [PubMed: 15058774]

43. Henry A, Charpiat B, Perol M, Vial T, de Saint Hilaire PJ, Descotes J. Paclitaxel hypersensitivity reactions: assessment of the utility of a test-dose program. Cancer J. 2006; 12:237–245. [PubMed: 16803683]

44. Silva GA. Nanotechnology applications and approaches for neuroregeneration and drug delivery to the central nervous system. Ann N Y Acad Sci. 2010; 1199:221–230. [PubMed: 20633128]

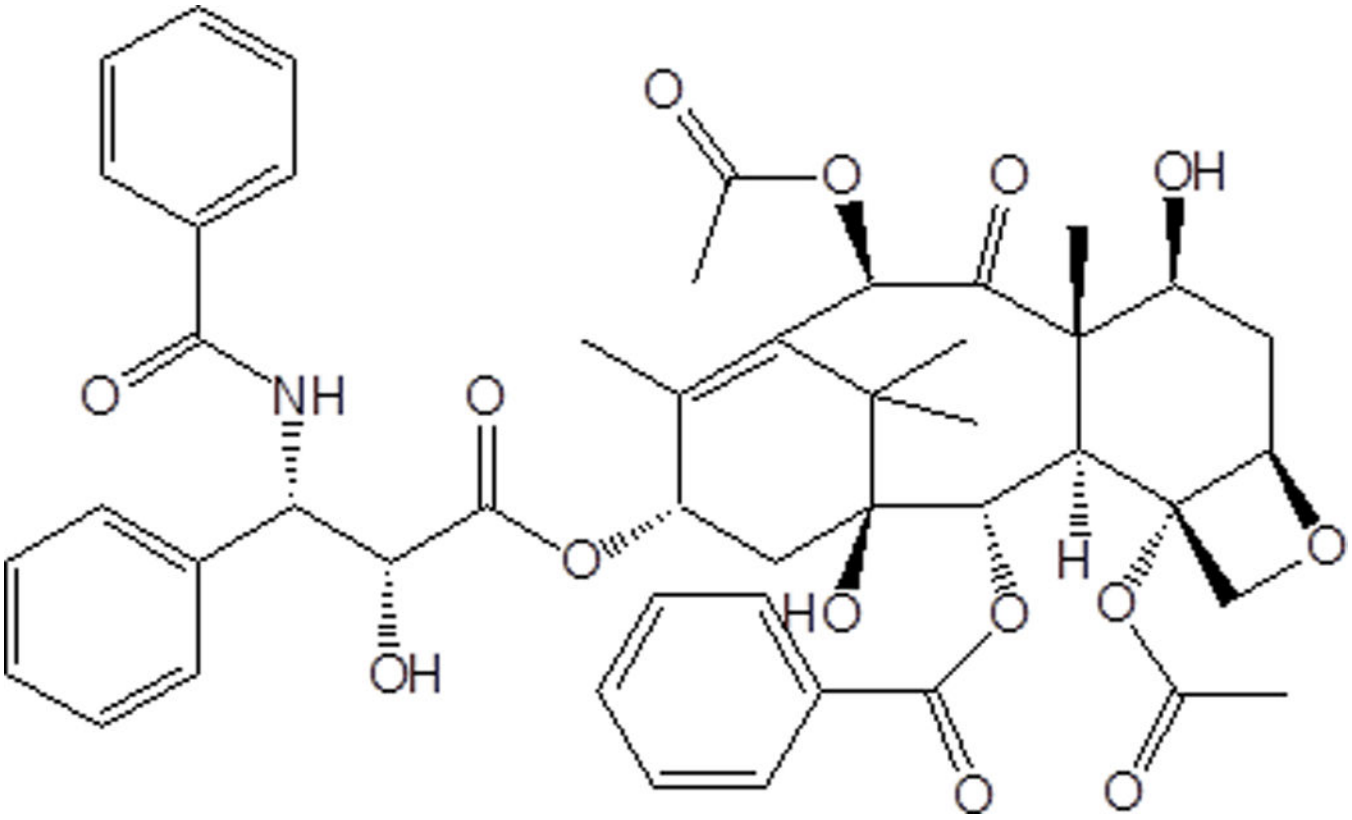

Figure 1.
Structure of paclitaxel, a diterpene chemotherapeutic agent isolated from the Pacific Yew (*Taxus brevifolia*) tree bark.

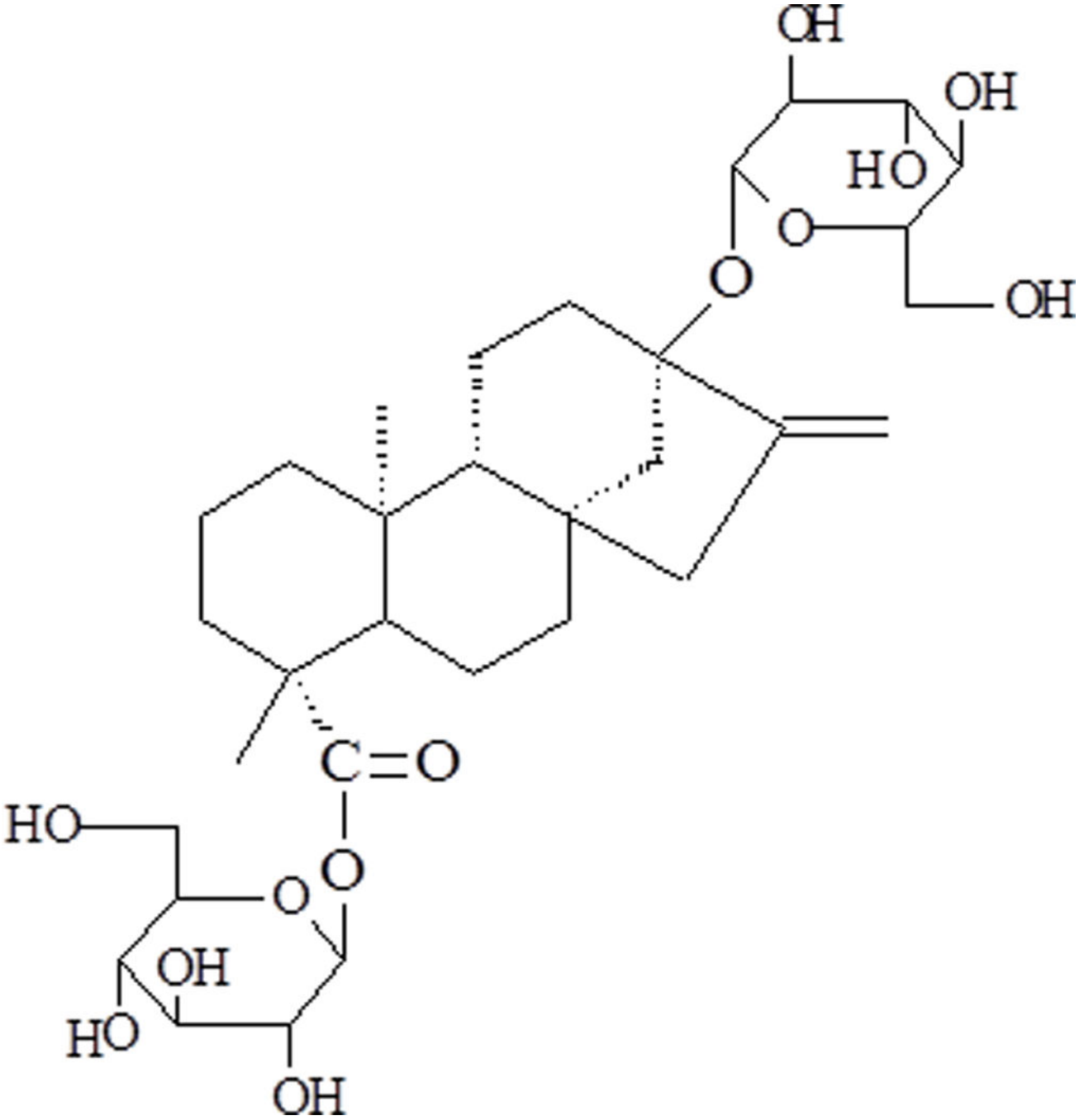

Figure 2.
Structure of rubusoside, a steviol glycoside used as a natural solubilizer isolated from the Chinese sweet tea plant (*Rubus suavissimus*).

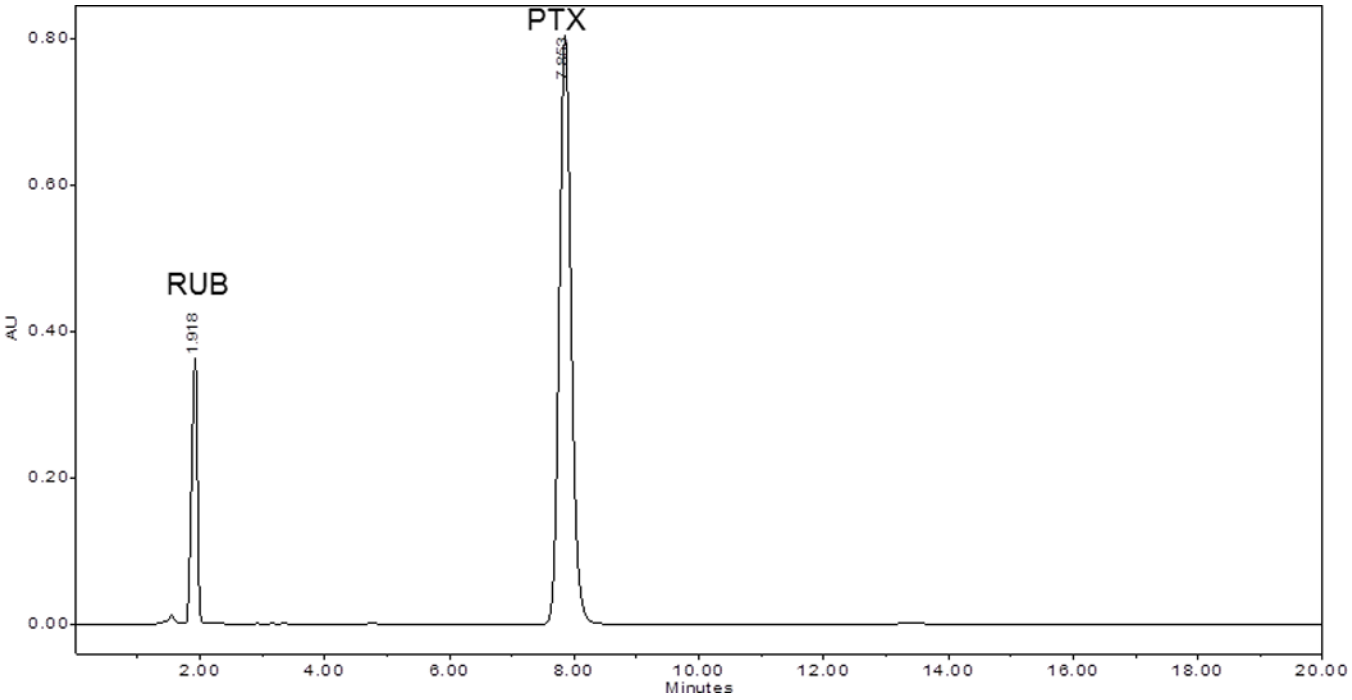

Figure 3.

Chromatogram of paclitaxel water solution acquired at 230 nm containing paclitaxel (PTX) and rubusoside (RUB) in a weight ratio of 1:50 PTX:RUB.

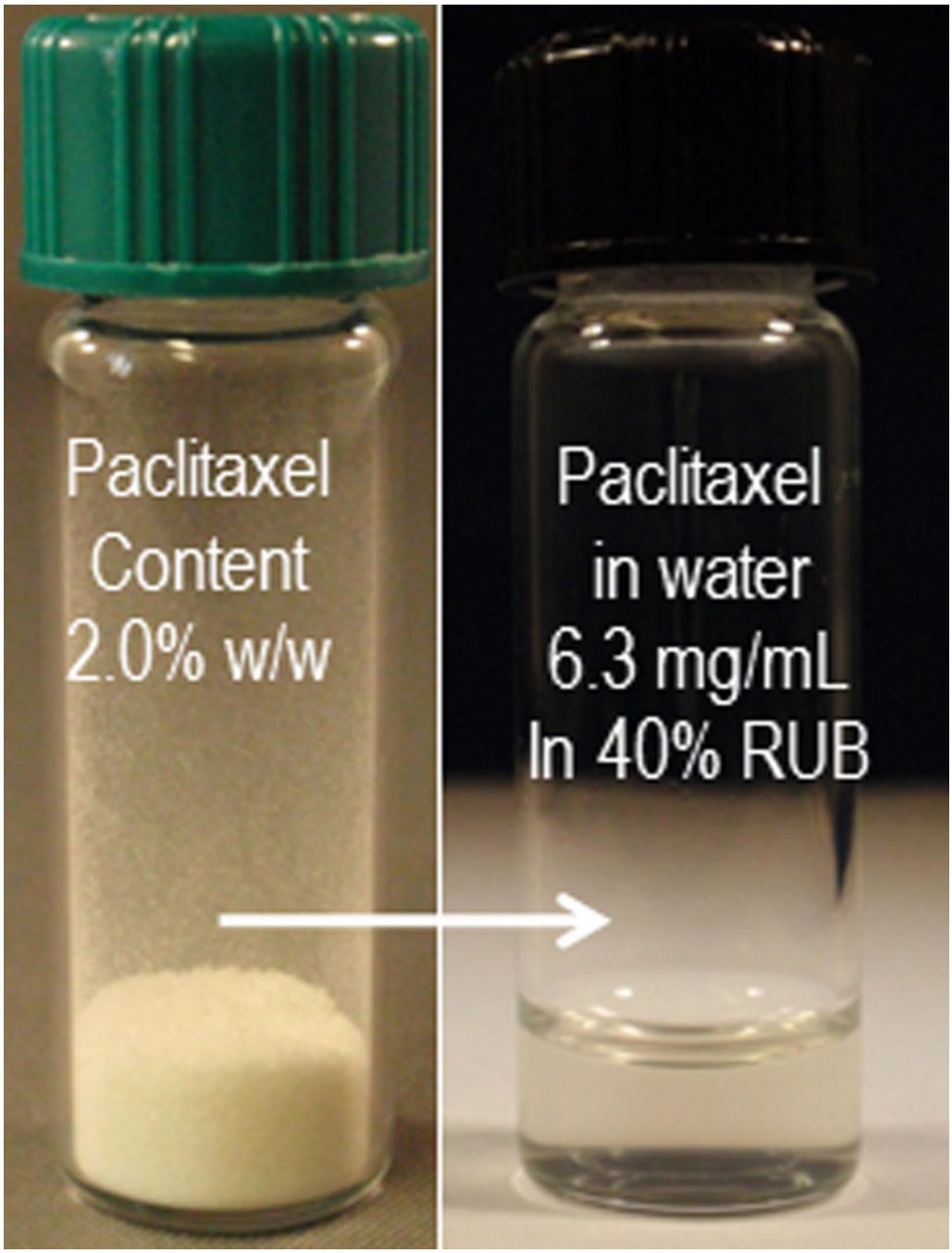

Figure 4.
PTX-RUB powder containing 2% of PTX was completely reconstituted to a clear water solution.

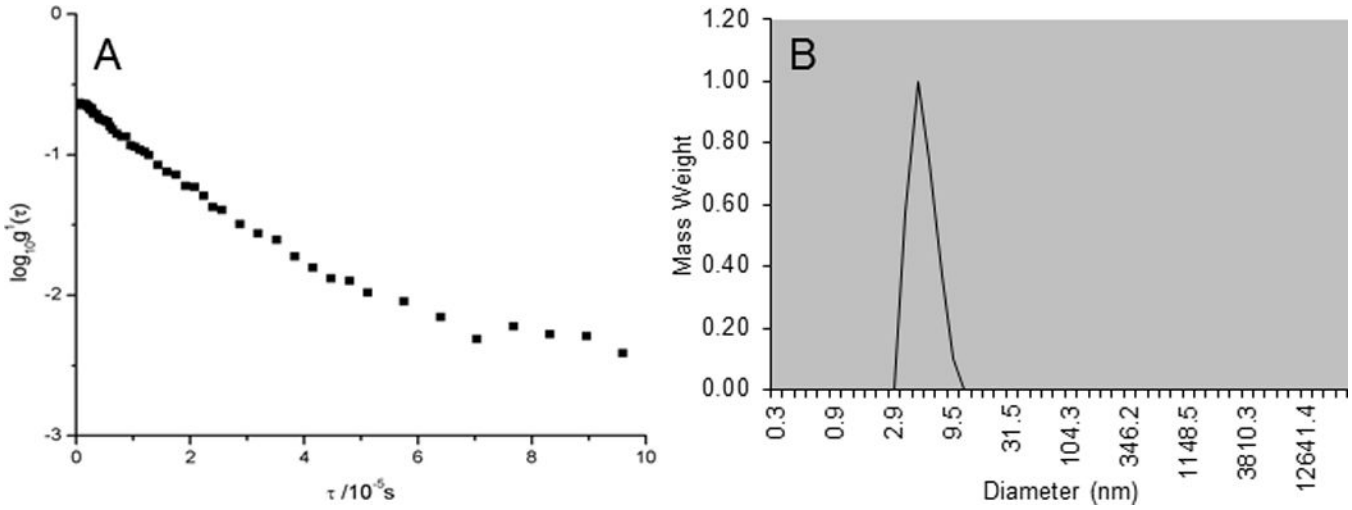

Figure 5.

Semilogarithmic plot (A) of normalized first-order autocorrelation function for 10% w/v RUB-solubilized paclitaxel water solution indicating a predominate monodispersion and particle size distribution (B) of PTX-RUB with 10% rubusoside in water measured by DLS with an average diameter of 7 nm.

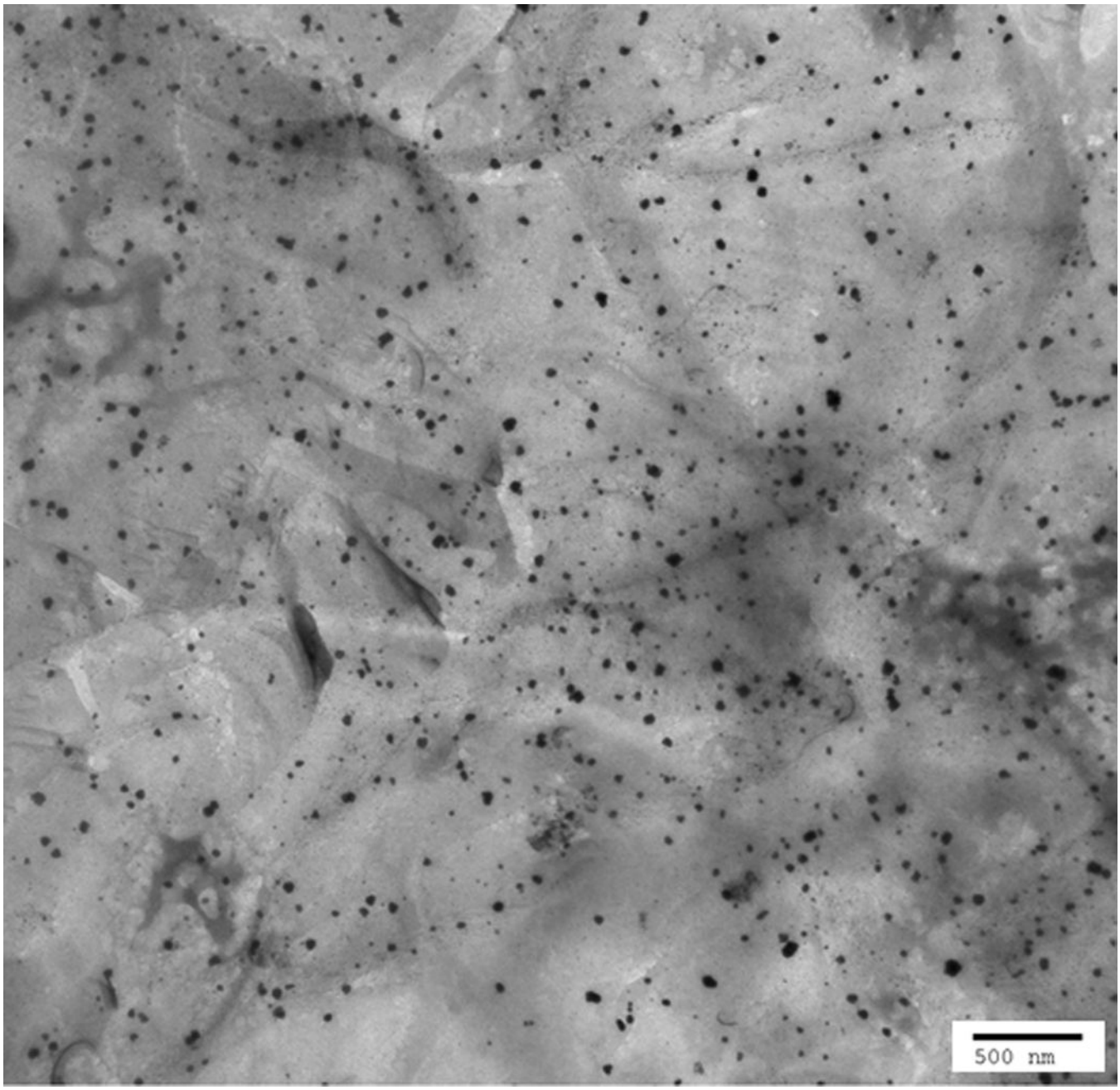

Figure 6.
FF-TEM image of PTX-RUB complexes shown as spherical particles (dark spots in the background of slide material).

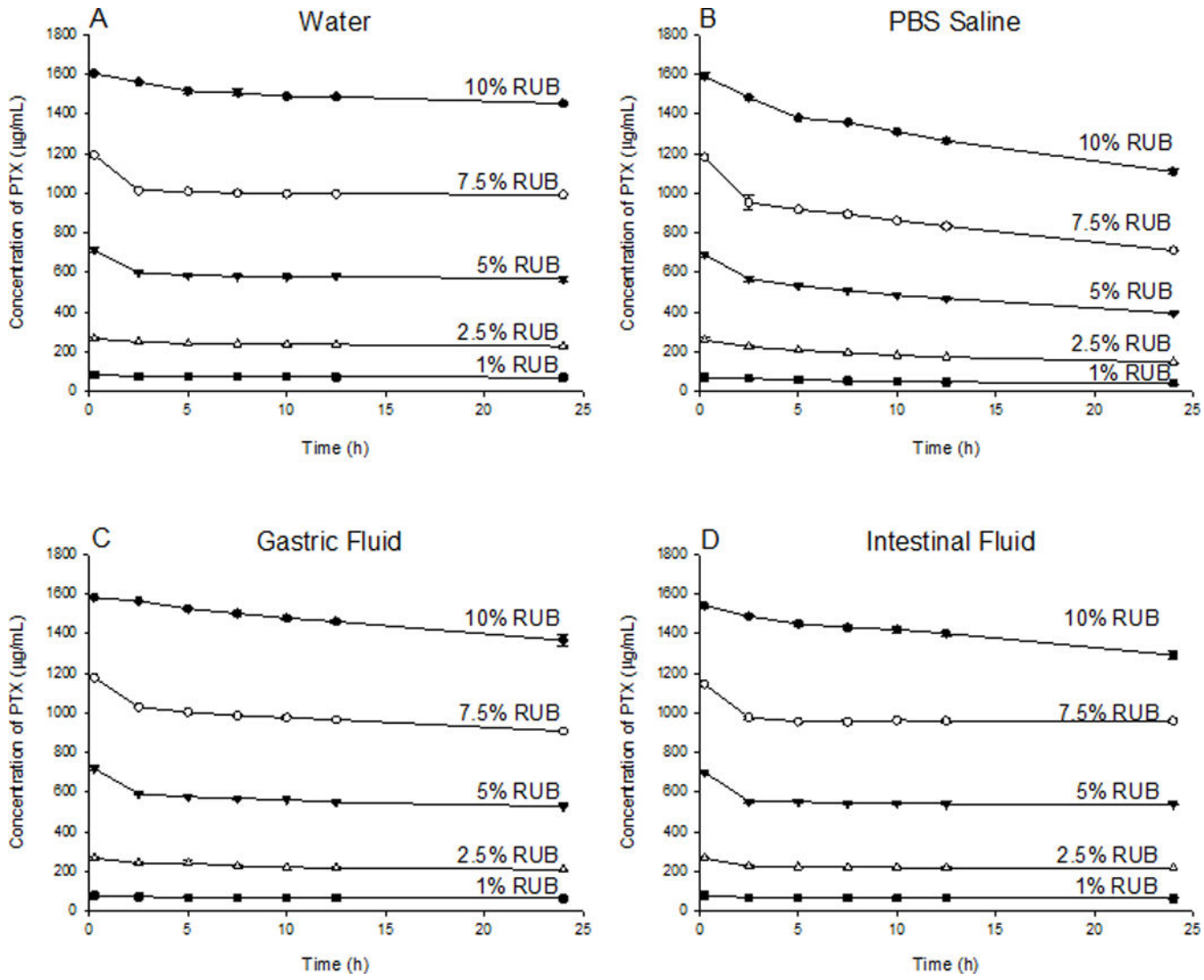

Figure 7.

Stability of PTX in physiological solutions and its response to dilution by a factor of 1.3, 2, 4 and 10 over 24 hrs following sample preparation at 37 °C. Each Data point represents the mean of three replicates ±SD.

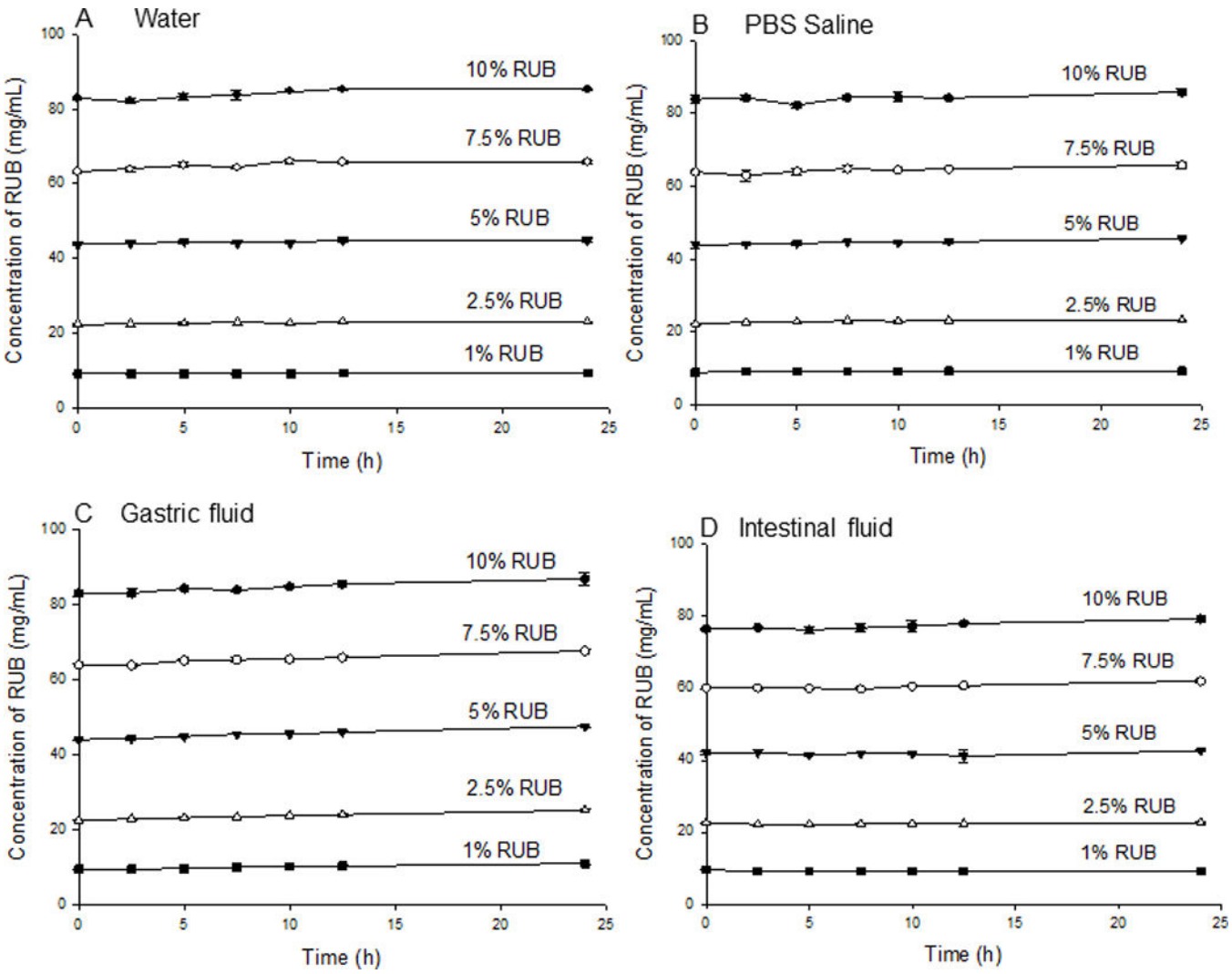

Figure 8.

Stability of RUB in physiological solutions and its response to dilution by a factor of 1.3, 2, 4 and 10 over 24 hrs following sample preparation at 37 °C. Each Data point represents the mean of three replicates ±SD.

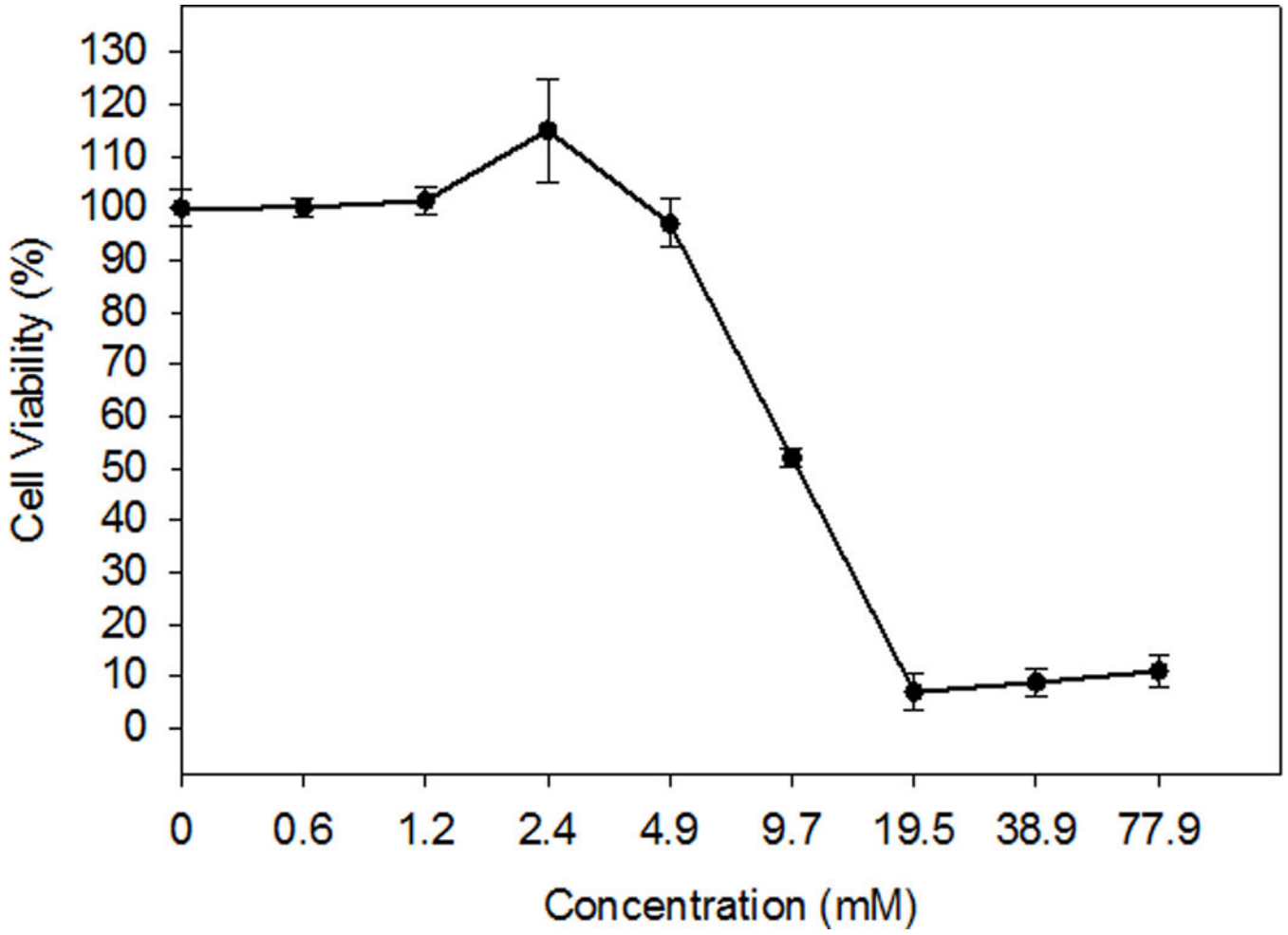

Figure 9.

Cell viability of Caco-2 cells influenced by RUB. Each data point represented the mean of two independent experiments with 3 wells in each experiment ±SE.

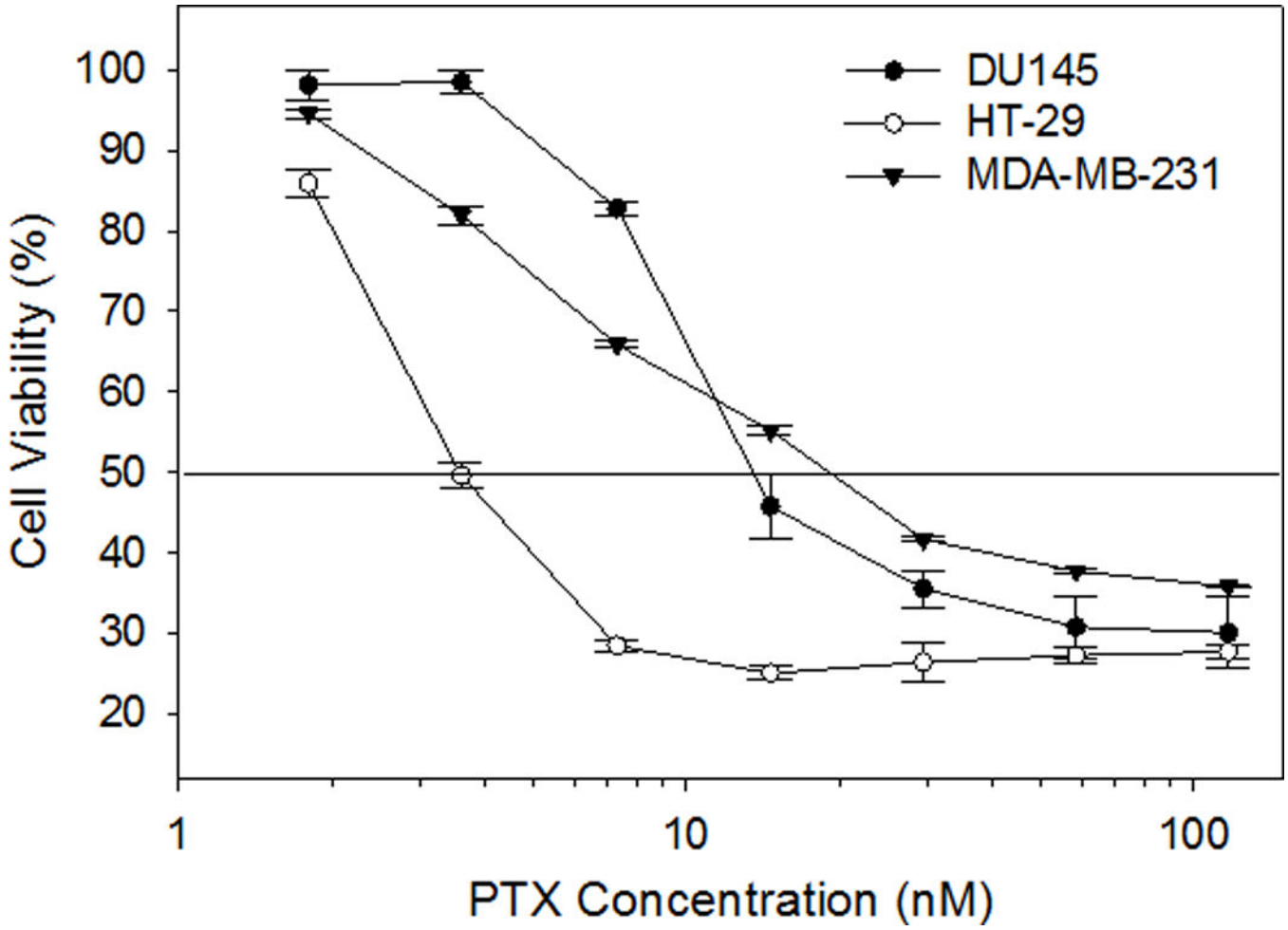

Figure 10.

Cell viability influenced by PTX-RUB. The horizontal line indicates 50% cell viability. Data points represent the mean obtained from two independent experiments ± SE.

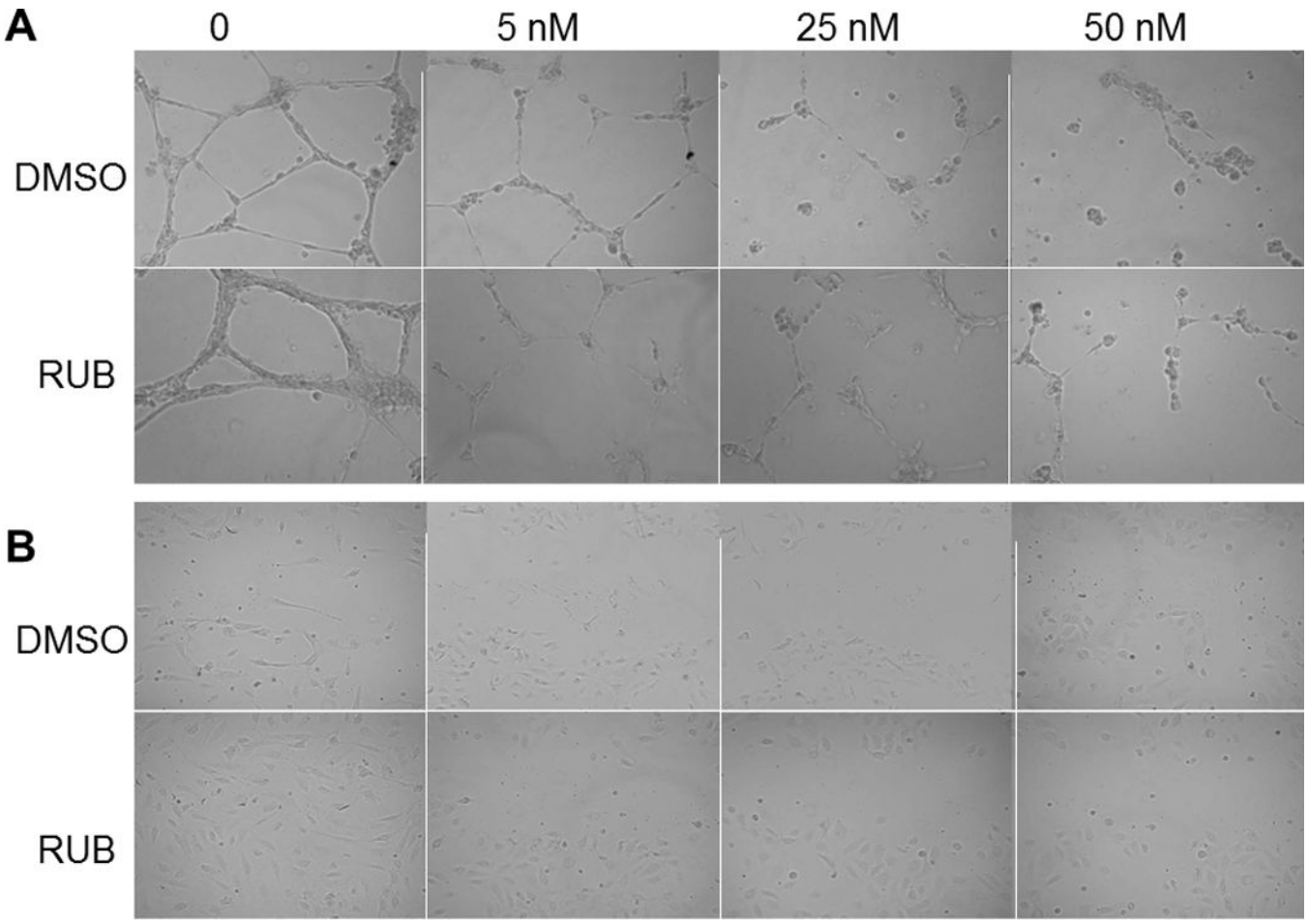

Figure 11.

Angiogenic responses of human umbilical vascular endothelial cells (HUVEC) to PTX treatment. A. HUVECs treated for 24 hrs by PTX at 0 (vehicle control), 5 nM, 25 nM, and 50 nM in the DMSO or RUB solubilization systems. B. Migration assay of HUVEC stimulated with 4 ng/mL vascular endothelial growth factor. HUVECs were scraped from the center and treated for 6 hrs by PTX at 0 (vehicle control), 5 nM, 25 nM, and 50 nM in the DMSO or RUB solubilization systems.

Table 1

PTX water solutions (mean ± SD; n=3) prepared from the reconstitution of PTX-RUB powder

Solution ID	Powder Weight (mg)	Water added (mL)	Final RUB concentration (mg/mL)	Final PTX concentration (μg/mL)	pH of solution	Final volume of the water solution (mL)
PTX-RUB1	10.14±0.13	1.00	10.0±0.1	76.3±1.3	5.66±0.02	1.00
PTX-RUB2.5	25.08±0.03	1.00	24.5±0.1	264.8±1.1	5.98±0.03	1.01
PTX-RUB5	50.13±0.07	1.00	48.0±0.2	660.1±5.5	6.10±0.02	1.04
PTX-RUB7.5	75.11±0.08	1.00	70.2±0.1	1101.2±5.0	6.19±0.02	1.07
PTX-RUB10	100.01±0.02	1.00	90.9±0.2	1567.2±9.8	6.22±0.01	1.09
PTX-RUB20	204.12±0.09	1.00	198.1±0.4	3536.1±10.1	6.34±0.01	1.11
PTX-RUB40	408.33±0.02	1.00	398.12±0.3	6258.2±12.3	6.08±0.04	1.15

Table 2

The reconstitution of PTX-RUB powder in physiological solutions

Sample	PTX-RUB added (mg)	Solvent added (mL)	RUB detected in solution (mg/mL)	PTX detected in solution (μg/mL)	pH
PTX-H_2O	300.02±0.02	3.0	92.5±0.6	1604±6	6.20±0.01
PTX-saline solution	300.07±0.01	3.0	93.0±0.6	1592±15	7.21±0.01
PTX-gastric fluid	300.00±0.01	3.0	94.0±0.2	1583±1	1.12±0.01
PTX-intestinal fluid	300.03±0.03	3.0	90.4±0.3	1542±9	5.75±0.01

Table 3

Permeability of PTX in the PTX-RUB formulation or the Taxol® formulation in Caco-2 cell monolayer

Formulation	Composition	Assay duration (hr)	P_{app}(A-B) (10^{-6}.cm.s^{-1})	Permeation enhancement
PTX-RUB	60 μg/mL PTX and 3 mg/mL RUB	2	3.83 ± 0.218	3.47
PTX-Taxol	60 μg/mL PTX, 5.2 mg/mL Cremophor EL, 50 μL/mL ethanol	2	1.10 ± 0.160	1.00

Table 4

Cytotoxicity expressed as mean IC_{50} ± standard error of PTX solubilized in RUB or DMSO

Cell Line	IC_{50} (nM)[1]	
	PTX in 1% DMSO	PTX-RUB in H_2O
HT-29 (Colon)	3.24 ± 0.34a[2]	3.77 ± 0.26a
MDA-MB-231 (Breast)	18.02 ± 1.28a	20.22 ± 1.77a
DU145 (Prostate)	12.77± 2.87a	15.49 ± 3.04a

[1] Each value represents the average of two independent experiments.

[2] Same letters following each IC_{50} value in each cell line indicate no significant differences ($P > 0.05$) by the Student's T-test.

Table 5

Characteristics of some paclitaxel nanoparticles

Formulation	Composition	Particle size (nm)	Solubility (mg/mL)	Reference
Paclitaxel PVP-b-PDLLA nanoparticles	Poly(N-vinylpyrrolidone)-block-poly(d,l-lactide)	56 or 16	≥2.5	[16]
Paclitaxel PDLLA-MePEG micelles	Amphiphilic diblock copolymer of poly (D,L- lactide)-block-methoxy polyethylene glycol	<50	5	[17]
Paclitaxel PEG-*b*-P(VBODENA) micelles	Diblock copolymer of poly(ethylene glycol) (PEG)- *b*-poly(2-(4-vinylbenzyloxy)-*N*,*N*- diethylnicotinamide)	105	≥38.9	[18]
Paclitaxel-PEG_{2000}-PE/TPGS micelles	Poly(ethylene glycol)2000–phosphatidyl ethanolamine conjugate d-α-tocopheryl polyethylene glycol 1000 succinate	14–15	5	[19]
Paclitaxel-PEG-HCCs formulation	PEGylated hydrophilic carbon clusters	<40	1.6	[20]
Paclitaxel-Pluronic P123 micelles	Pluronic P123	25	≥0.3	[21]
Paclitaxel-Pluronic F127 Nanocrystal	Pluronic F127	122	≥2	[22]
Paclitaxel-DHC micelles	N-deoxycholic acid-N, O-hydroxyethyl chitosan	200–240	≥2	[23]
Cremophor EL	Cremophor EL, ethanol	0	≥6.3	[24]
PTX-RUB	RUB	7	6.3	This study